Chapter 3

Two Proposed Techniques of Fully-Balanced, High-Q, Wide-Dynamic-Range, Current-Tunable Gm-C Bandpass Filters

3.1 Introduction

Chapter 3 develops two proposed techniques 1 and 2 of fully balanced high-Q wide-dynamic-range current-tunable Gm-C bandpass filters. The techniques are relatively simple based on three fully balanced components, i.e. an adder, a low-Q-based bandpass filter or an amplifier. Technique 1 proposes a fully balanced high-Q wide-dynamic-range current-tunable Gm-C bandpass filter I where the high-Q factor is approximately equal to a typically high and constant value of a common-emitter current gain (β) and is, for the first time, independent of variables such as a center frequency. Technique 2 proposes a fully balanced high-Q wide-dynamic-range current-tunable Gm-C bandpass filter II where the high-Q factor is possible through a tunable bias current.

This chapter can be separated into seven sections. Section 3.2 proposes a possible system realization of a high-Q bandpass filter. Following the system realization, circuit realizations through Examples 1 and 2 of the fully balanced high-Q current-tunable Gm-C bandpass filters are presented in Sections 3.3 and 3.4, respectively. Section 3.5 describes sensitivities whilst Section 3.6 describes dynamic ranges (DRs) of the Gm-C bandpass filters. Finally, conclusions are drawn in Section 3.7.

3.2 Proposed System Realization of a High-Q Bandpass Filter

Figure 3.1 shows the proposed system realization of a high-Q bandpass filter where the system is relatively simple based on three fully balanced components, i.e. a two-input adder A_D, an amplifier A_G and a low-Q-based bandpass filter $A_{LQ}(s)$.

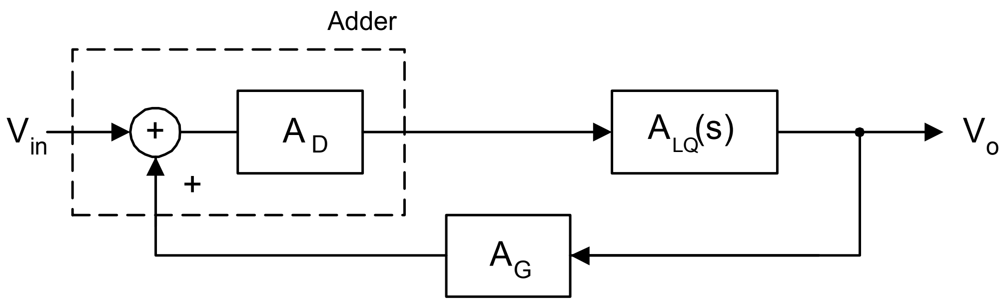

Figure 3.1 Proposed system realization of a high-Q bandpass filter

The standard transfer function of any 2nd order bandpass filter $A_{LQ}(s)$ can be written as:

$$A_{LQ}(s) = \frac{a_1(\frac{\omega_o}{Q_{LQ}})s}{s^2 + \frac{\omega_o}{Q_{LQ}}s + \omega_o^{\ 2}} \tag{3.1}$$

where a_1 is a pass band gain, i.e. $a_1 = A_{LQ}(s)$ at $s = j\omega_o$ and Q_{LQ} is a relatively low-Q factor of $A_{LQ}(s)$. Consequently, a closed-loop gain $A_{HQ}(s) = v_o/v_{in}$ is given by

$$A_{HQ}(s) = \frac{A_D A_{LQ}(s)}{1 - A_D A_G A_{LQ}(s)} \tag{3.2}$$

Substituting $A_{LQ}(s)$ in (3.2) with (3.1) yields

$$A_{HQ}(s) = \frac{A_D a_1(\frac{\omega_o}{Q_{LQ}})s}{s^2 + \frac{\omega_o}{Q_{HQ}}s + \omega_o^{\ 2}} \tag{3.3}$$

where the quality factor Q_{HQ} is given by

$$Q_{HQ} = \frac{Q_{LQ}}{1 - A_D A_G a_1} \tag{3.4}$$

It can be seen from (3.4) that Q_{HQ} may ideally approach infinite if the denominator (1 – $A_D A_G a_1$) approaches zero. In other words,

$$A_G \rightarrow \frac{1}{a_1 A_D} \tag{3.5}$$

In practice, the denominator of (3.4) may be made relatively small, i.e. A_G is in the proximity of $1/(a_1 A_D)$, resulting in a relatively high quality factor Q_{HQ}.

3.3 Proposed Circuit Realization using Technique 1: A Fully Balanced High-Q Current-Tunable Gm-C Bandpass Filter I.

3.3.1 Circuit Description of Technique 1

Figure 3.2 shows the proposed circuit realization for Figure 3.1 through a technique 1 called a fully balanced high-Q current-tunable Gm-C bandpass filter I (A_{HQ1}). The circuit consists of two fully balanced components, i.e. a two-input adder (A_D) and a low-Q-based bandpass filter (A_{LQ}) whilst the amplifier A_G = 1 (i.e. a direct connection), using matched transistors T1 to T10. In this case, equation 3.5 suggests that the gain of the adder $A_D \cong 1$ and the passband gain $a_1 \cong 1$.

Firstly, the adder A_D is a modified version of an existing adder (Srisuchinwong, 2000) and consists of a differential pair (T1, T2), a common-collector pair (T3, T4) and a current sink $2I_1$. For example, the current sink I_x may be implemented by a resistor (R) and two trasistors (Tx and Ty) as shown in Figure 3.2. The 1st small-signal input voltage of A_D is v_{AB}

between the bases of T1 and T2 (or nodes A and B). The 2nd small-signal input voltage of A_D is v_{CD} between the bases of T3 and T4 (or nodes C and D). A small-signal output voltage of A_D is v_{EF} between the emitters of T3 and T4 (or nodes E and F).

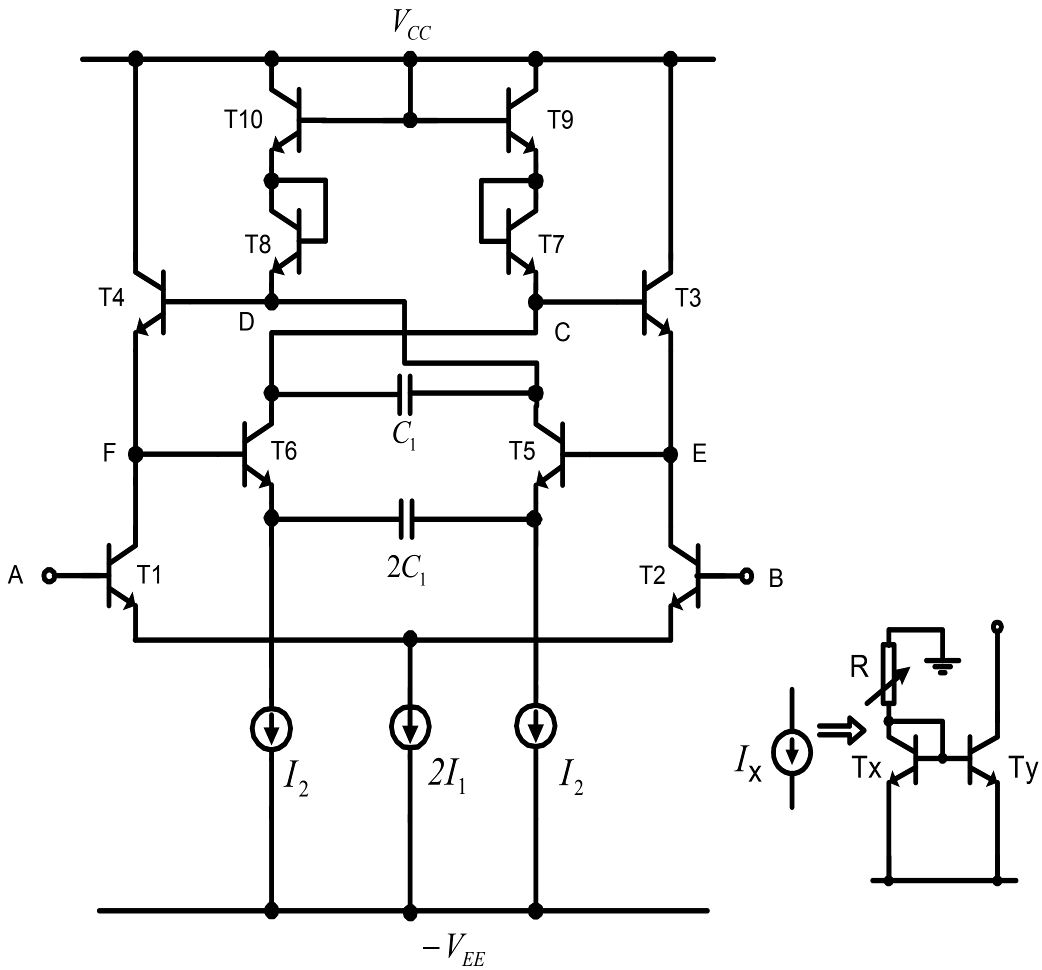

Figure 3.2 Proposed circuit realization using Technique 1:

A fully balanced high-Q current-tunable Gm-C bandpass filter I.

Secondly, the low-Q-based bandpass filter A_{LQ} is a modified version of an existing low-Q bandpass filter (Pookaiyaudom, et al., 1987) and consists of a differential pair (T5, T6), two capacitors C_1 and $2C_1$, two current sinks I_2 and four loading diode-connected transistors T7 to T10. A small-signal input voltage of A_{LQ} is v_{EF} between the bases of T5 and

T6 (or nodes E and F) and is obtained from the output v_{EF} of A_D. A small-signal output voltage of A_{LQ} is v_{CD} between the emitters of T7 and T8 (or nodes C and D). Finally, the transfer function of the high-Q bandpass filter is $A_{HQ1} = v_O / v_{in}$ where $v_{in} = v_{AB}$ and $v_O = v_{CD}$. It can be seen from Figure 3.2 that the circuit is fully balanced.

3.3.2 A Current-Tunable Gm-C Bandpass Filter (A_{HQ1})

Parameters r_{e1}, r_{e2}, …, r_{e9} and r_{e10} are the small-signal emitter resistance of transistors T1, T2, …, T9 and T10, respectively, where $(r_{e1} = r_{e2}) = V_T/I_1$, $(r_{e3} = r_{e4}) \cong V_T/(\alpha I_1) \cong r_{e1}/\alpha$, $(r_{e5} = r_{e6}) = V_T/I_2$, $(r_{e7} = r_{e8} = r_{e9} = r_{e10}) \cong V_T/(\alpha I_2) \cong r_{e5}/\alpha$ for $\alpha = \beta/(\beta+1)$ and β is the common-emitter current gain of a BJT. The usual thermal voltage V_T is approximately 25 mV associated with an pn junction at room temperature.

Firstly, the two-input adder A_D is considered. The output v_{EF} of A_D is obtained through superposition, i.e. $v_{EF} = v_{O1} + v_{O2}$. The voltage v_{O1} is the output v_{EF} of A_D when the 1^{st}-input v_{AB} of A_D is activated, i.e. $v_{AB} = v_{in}$, but the 2^{nd}-input v_{CD} of A_D is temporary deactivated or separately connected to an ac ground, i.e. $v_{CD} = 0$. In contrast, the voltage v_{O2} is the output v_{EF} of A_D when the 2^{nd}-input v_{CD} of A_D is activated, i.e. $v_{CD} = v_O$, but the 1^{st}-input v_{AB} of A_D is temporary deactivated or connected to an ac ground, i.e. $v_{AB}=v_{in}= 0$.

On the one hand, v_{O1} can be found at $v_{CD} = 0$. Therefore, v_{in} of A_D enables a small-signal emitter current $i_{e1} = v_{in}/(2r_{e1})$ passing through the emitters of T1 and T2. The resulting small-signal collector current of T1 and T2 is $i_{c1}=\alpha i_{e1}$. Most of i_{c1} passes through a loading impedance $Z_1 = 2r_{e3}$ formed by T3 and T4. As $v_{O1} \cong i_{c1}Z_1$, therefore $v_{O1}/v_{in} \cong 1$. Consequently, $v_{O1} \cong v_{in}$.

On the other hand, v_{O2} can be found at $v_{in} = 0$. Therefore, the gain of the common-collector pair (T3, T4) is $v_{O2} / v_{CD} \cong 1$, or $v_{O2} \cong v_{CD}$. Consequently, $v_{EF} = v_{O1} + v_{O2} \cong v_{in} + v_{CD}$, i.e. the gain of the adder $A_D \cong 1$. As $v_{CD} = v_O$, therefore

$$v_{EF} \cong v_{in} + v_O \tag{3.6}$$

Secondly, the low-Q-based bandpass filter A_{LQ} is considered. The input v_{EF} of A_{LQ} enables a small-signal emitter current $i_{e2} = v_{EF}\,(2sC_1)/(1+s\tau_1)$ passing through the emitters of T5 and T6, where $\tau_1 = 4r_{e5}C_1$. The resulting small-signal collector current of T5 and T6 is $i_{c2} = \alpha i_{e2}$. Most of i_{c2} passes through a loading impedance $Z_2 = 4r_{e7}/(1+s\tau_2)$ formed by T7 to T10 where $\tau_2 = 4r_{e7}C_1$ and therefore $\tau_2 \cong \tau_1/\alpha$. The resulting output of A_{LQ} is $v_{CD} \cong i_{c2}Z_2$, therefore $A_{LQ} = v_{CD} / v_{EF} = v_O / v_{EF}$ represents a low-Q-based bandpass filter A_{LQ} of the form

$$A_{LQ} = \frac{v_O}{v_{EF}} = \frac{2s\alpha/\tau_1}{s^2 + (1+\alpha)\frac{s}{\tau_1} + \frac{\alpha}{\tau_1^2}} \tag{3.7}$$

The center frequency of (3.7) is $\omega_{LQ} = (\alpha^{1/2})/\tau_1$. The quality factor of (3.7) is $Q_{LQ} = (\alpha^{1/2}) / (1+\alpha) \cong 0.5$ which is a relatively low value. It can be seen from (3.1) and (3.7) that $a_1 = 2\alpha / (1+\alpha) \cong 1$. In other words, at $s = j\omega_{LQ}$, the passband gain of (3.7) is $A_{LQ} = a_1 = 2\alpha / (1+\alpha) \cong 1$.

Finally, the high-Q bandpass filter A_{HQ} can be considered by substituting v_{EF} in (3.7) with (3.6), therefore $A_{HQ1} = v_O / v_{in} \cong A_{LQ} / (1-A_{LQ})$, i.e.

$$A_{HQ1} = \frac{v_o}{v_{in}} = \frac{2\alpha s/\tau_1}{s^2 + (1-\alpha)\frac{s}{\tau_1} + \frac{\alpha}{\tau_1^2}} \tag{3.8}$$

The center frequency of (3.8) is $\omega_{HQ} = (\alpha^{1/2}) / \tau_1 = g_{m5} / [(\alpha^{1/2})\ 4C_1]$ where the transconductance $g_{m5} = \alpha / r_{e5}$. At $s = j\omega_{HQ}$, the passband gain of (3.8) is ideally (i.e. without loading effect) $A_{HQ}(s) = 2\alpha / (1-\alpha) \cong 2\beta$ which is much greater than the passband gain of (3.7) where $A_{LQ} = a_1 = 2\alpha / (1+\alpha) \cong 1$ at $s = j\omega_{LQ}$. The center frequency ω_{HQ} is current tunable by I_2 of the form

$$\omega_{HQ} = \frac{I_2}{4C_1V_T}\sqrt{\frac{\beta}{\beta+1}} \tag{3.9}$$

3.3.3 A Typically High and Constant Quality Factor (Q_{HQ1})

The quality factor of (3.8) is $Q_{HQ1} = (\alpha^{1/2}) / (1-\alpha)$ and therefore

$$Q_{HQ1} \cong \beta \tag{3.10}$$

The quality factor Q_{HQ1} of the proposed Technique 1 is approximately equal to a typically high (>100) and constant value of the current gain β and is, for the first time, no longer a function of variables such as a center frequency. The typically constant quality factor Q_{HQ} results in not only a great reduction in the need for additional or complicated tunable circuits, but also a much better sensitivity of the Q factor.

Variations of Q_{HQ1} with temperature may be expected, as β may depart from its typically constant value due to temperature. Such variations, however, are relatively much smaller and slower than the variations of most reported Q factors which have generally been a function of variables such as a center frequency (Comer et al., 1997 and Ali et al., 2000) or have particularly been inversely proportional to the center frequency (Liu and Karsilayan, 2003 and Voghell and Sawan, 2000).

In addition, possible solutions for good stability of the quality factor Q_{HQ} with temperature could be suggested through the use of, for example, InGaP/GaAs Heterojunction Bipolar Transistors (HBTs) where a relatively constant current gain β has been reported as a function of temperature up to 300°C (Bashar, et al., 1996), or through the use of $Al_XGa_{0.52-X}In_{0.48}P$/GaAs HBTs where good stability of β with collector current and temperature has been demonstrated for X = 0.18-0.30 (Ho-Kwang, et al., 1996).

3.4 Proposed Circuit Realization using Technique 2 : A Fully Balanced High-Q Current-Tunable Gm-C Bandpass Filter II.

3.4.1 Circuit Description of Technique 2

Figure 3.3 shows an alternative circuit realization for Figure 3.1 through a technique 2 called a fully balanced, high-Q current-tunable Gm-C bandpass filter II (A_{HQ2}). As shown in Figure 3.3, a differential amplifier A_G is added to the circuit diagrams of Figure 3.2, where the A_G is formed by transistors T11 and T12, a current sink $2I_3$ and two loading resistors R_C. For example, the current sink I_x may be implemented by a resistor (R) and two trasistors (Tx and Ty) as shown in Figure 3.3.

The small-signal input voltage of A_G is v_{GH} between the bases of T11 and T12 (or nodes G and H) and is obtained from the output v_{GH} of A_{LQ}. The small-signal output voltage of A_G is v_{CD} between the collectors of T12 and T11 and is applied to the 2^{nd}-input v_{CD} of A_D. The transfer function of the high-Q bandpass filter is $A_{HQ2} = v_O / v_{in}$ where $v_{in} = v_{AB}$ and $v_O = v_{CD}$. It can be seen from Figure 3.3 that the circuit is also fully balanced.

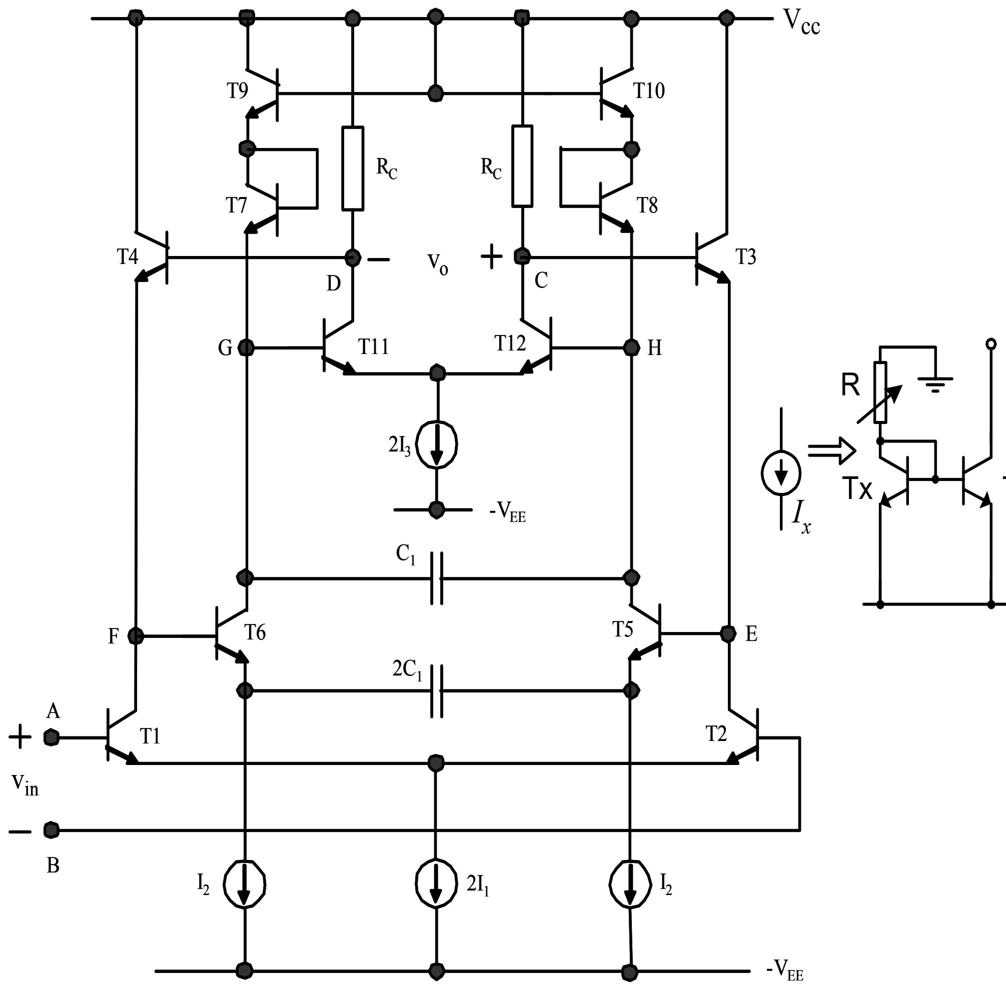

Figure 3.3 Proposed circuit realization using Technique 2:

A fully balanced high-Q current-tunable Gm-C bandpass filter II.

3.4.2 A Current-Tunable Gm-C Bandpass Filter (A_{HQ2})

The input v_{GH} of A_G enables a small-signal emitter current $i_{e3} = v_{GH}/(2r_{e11})$ passing through the emitters of T11 and T12 where $r_{e11} = V_T/I_3$ is the small-signal emitter resistance of either T11 or T12. The resulting small-signal collector current of T11 and T12 is $i_{c3} = \alpha i_{e3}$. Most of i_{c3} passes through a loading resistance $Z_3 = 2R_C$. The resulting output of A_G is $v_{CD} \cong i_{c3}Z_3$, and $v_{CD} = v_O$ therefore

$$A_G = \frac{v_O}{v_{GH}} = \frac{\alpha R_C}{r_{e11}} \qquad (3.11)$$

In a similar fashion to (3.8), the high-Q current-tunable bandpass filter $A_{HQ2} = v_O / v_{in} \cong A_G A_{LQ} / (1 - A_G A_{LQ})$, i.e.

$$A_{HQ2} = \frac{v_o}{v_{in}} = \frac{2\alpha A_G s/\tau_1}{s^2 + (1 + \alpha - 2\alpha A_G)\frac{s}{\tau_1} + \frac{\alpha}{\tau_1^2}} \qquad (3.12)$$

The center frequency ω_{HQ} of (3.12) is $\omega_{HQ} = (\sqrt{\alpha}) / \tau_1$ and is current tunable by I_2, as shown in (3.9).

3.4.3 A Current-Tunable High Quality Factor (Q_{HQ2})

The quality factor of (3.12) is $Q_{HQ2} = (\alpha^{1/2}) / (1 + \alpha - 2\alpha A_G)$. As $\alpha \cong 1$, therefore Q_{HQ2} is current tunable by I_3 of the form

$$Q_{HQ2} \cong \frac{1/2}{(1 - A_G)} \cong \frac{1/2}{(1 - \frac{R_C I_3}{V_T})} \qquad (3.13)$$

Equation (3.13) is comparable to (3.4) where $Q_{LQ} = 0.5$, $a_1 A_D = 1$ and $A_G = I_3 R_C / V_T$. It may be suggested from (3.13) that the quality factor Q_{HQ2} ideally approaches infinite at $A_G = 1$ or $I_3 = V_T / R_C$. In practice, however, Q_{HQ2} should be current tunable to a relatively large value through I_3 where I_3 is in the proximity of V_T / R_C.

3.5 Sensitivities of the Two Proposed Gm-C Bandpass Filters in Techniques 1 and 2

Sensitivities are important parameters where circuit configurations may be compared for establishing practical utilities in meeting desired requirements. Calculations of sensitivities allow designers to select better circuits or permit conclusions whether a chosen filter satisfies or will keep satisfying the given specifications. Generally, a sensitivity of y to a variation of x is given by $S_x^y = [\partial y/\partial x][x/y)]$ where y is a parameter of interest and x is a parameter of variation. Appendix A shows the analytical treatments for the sensitivities of Techniques 1 and 2. Table 3.1 summaries sensitivity S_x^y of Technique 1 where (x, y) = (β, Q_{HQ1}), (C_1, ω_{HQ}), (V_T, ω_{HQ}), (I_2, ω_{HQ}) or (β, ω_{HQ}), and shows sensitivity S_x^y of Technique 2 where (x, y) = (R_C, Q_{HQ2}), (V_T, Q_{HQ2}), (I_2, Q_{HQ2}), (C_1, ω_{HQ}), (V_T, ω_{HQ}), (I_2, ω_{HQ}) or (β, ω_{HQ}). The thermal voltage V_T also represents effects of temperature on the centre frequency ω_{HQ} whilst the current gain β also represents effects of temperature on the quality factor Q_{HQ}. It can be concluded from Table 3.1 that:

(a) In Technique 1, the sensitivity of Q_{HQ1} to the variation of β and the sensitivities of ω_{HQ} to the variations of C_1, V_T, or I_2 are constant values either –1 or 1 and therefore, are desirably independent of parameters. Such sensitivities are, unlike existing approaches (Comer et al., 1997 and Ali et al., 2000), no longer strongly affected by the quality factor Q_{HQ1} or variables.

(b) In Technique 2, for very high-Q realizations (i.e. $I_3 \cong V_T/R_C$), the sensitivities of Q_{HQ2} to the variation of R_C, V_T, or I_3 are in the same order as those given in the literature (Comer et al., 1997 and Ali et al., 2000) whilst the sensitivities of ω_{HQ} to the variations of C_1, V_T, or I_2 are constant values from –1 to 1.

(c) In Techniques 1 and 2, for a large value of β, the sensitivity $S_\beta^{\omega_{HQ}} = 1/[2(\beta+1)]$ is not only relatively small (e.g. $S_\beta^{\omega_{HQ}} = 0.0041$ at $\beta = 120$) but also relatively constant because variations of a large β in the denominator of a small ratio 1/[2(β+1)] should not strongly affect the sensitivity $S_{\beta}^{\omega_{HQ}}$ (e.g. $S_{\beta}^{\omega_{HQ}}$ = 0.0035 at β = 140).

Table 3.1 Sensitivity S_x^y where (x,y) = (β, Q_{HQ1}), (R_C, Q_{HQ2}), (V_T, Q_{HQ2}), (I_2, Q_{HQ2}), (C_1, ω_{HQ}), (V_T, ω_{HQ}), (I_2, ω_{HQ}) or (β, ω_{HQ}).

	$S_{\beta}^{Q_{HQ1}}$	$S_{R_C}^{Q_{HQ2}}$	$S_{V_T}^{Q_{HQ2}}$	$S_{I_3}^{Q_{HQ2}}$	$S_{C_1}^{\omega_{HQ}}$	$S_{V_T}^{\omega_{HQ}}$	$S_{I_2}^{\omega_{HQ}}$	$S_{\beta}^{\omega_{HQ}}$
Technique 1 (Figure 3.2)	1.0	-	-	-	-1.0	-1.0	1.0	1/[2(β+1)]
Technique 2 (Figure 3.3)	-	-2Q_{HQ2}	2Q_{HQ2}	2Q_{HQ2}	-1.0	-1.0	1.0	1/[2(β+1)]

3.6 Dynamic Ranges (DRs) of the Two Proposed Gm-C Bandpass Filters in Techniques 1 and 2

Dynamic ranges (DRs) of either a specific biquad or an optimized high-Q biquad in a general way have been presented (Groenewold, 1991). An expression for the dynamic range of a second-order Gm-C biquad in a general way is given by (Groenewold, 1991):

$$DR = \frac{v_{\max}^2}{\overline{v_{noise}^2}} = \frac{v_{\max}^2}{kT\xi Q\left(\frac{1}{C_a} + \frac{1}{C_b}\right)} \qquad (3.14)$$

where $v_{\max}$ is the maximal signal level at the input or output of a system, $\overline{v_{noise}^2}$ is the mean squared noise voltage at the same point, C_a and C_b are two capacitors in the filter, k is the Boltzmann's constant, T is the absolute temperature, ξ is the noise factor of the transconductor (Gm) and Q is the quality factor. The dynamic range of the proposed technique can be improved by not only increasing $v_{\max}^2$, but also reducing $\overline{v_{noise}^2}$ of (3.14) as follows.

On the one hand, it is known that, the maximal signal level v_{max} of a fully balance circuit is typically twice the maximal signal level v_M of a single-ended circuit (Groenewold, 1991), i.e. $v_{max} \cong 2v_M$. In other words, the magnitude v_{max} of (3.14) may be double through the use of a fully balanced circuit. On the other hand, the mean squared noise voltage can be reduced through the use of a shunt positive feedback configuration providing enhanced current gain and thereby improving the overall noise. Table 3.2 summarizes values of C_a, C_b, and dynamic ranges (DRs) of the proposed Gm-C techniques and other existing Gm-C approaches (Groenewold, 1991; Kuhn et al., 2003).

Table 3.2 Dynamic ranges (DRs) and values of C_a, C_b, v^2_{max} of Techniques 1 and 2 of the two proposed fully balanced Gm-C techniques and those of other existing Gm-C approaches.

References	Capacitors	V_{max}	$DR = \dfrac{v^2_{max}}{kT\xi Q\left(\dfrac{1}{C_a}+\dfrac{1}{C_b}\right)}$
This work Techniques 1 and 2 (Figures 3.2 and 3.3) (fully balanced)	$C_a = C$ $C_b = 2C$	$2v_{M1}$	$DR_a = 2.67\dfrac{v^2_{M1}C}{(kT\xi Q)_1}$
Kuhn et al., 2003 (single ended)	$C_a = C$ $C_b = C$	v_{M2}	$DR_b = 0.50\dfrac{v^2_{M2}C}{(kT\xi Q)_2}$
Groenewold, 1991 (single ended)	$C_a = C/2$ $C_b = C/2$	v_{M3}	$DR_c = 0.25\dfrac{v^2_{M3}C}{(kT\xi Q)_3}$

It can be seen from Table 2 that if $v_{M1} = v_{M2} = v_{M3}$ and $(KT\xi Q)_1 = (KT\xi Q)_2 = (KT\xi Q)_3$, then $DR_1 > DR_2 > DR_3$. The proposed Gm-C fully-balanced technique can therefore enable a higher dynamic range DR_1, especially when $\overline{v^2_{noise}}$ is also additionally reduced. In particular, as the quality factor Q in (3.14) becomes Q_{HQ} which is no longer a function of variables such as a center frequency, the dynamic range DR_1 is therefore, unlike existing approaches (Groenewold, 1991; Kuhn et al., 2003), no longer strongly affected by those variables previously associated in the Q factor. As an example, it can be expected from Table 2 that DR_1 = 88.28 dB if $v_{max} = 2\ v_{M1}$ = 127 mV (i.e. -5 dBm through a 50-Ω load), v_{M1} = 63.5 mV, $kT\xi = 2\times10^{-23}$ (Kuhn et al., 2003), Q = 120 and C = 150 pF.

3.7 High Frequency Responses of the Two Proposed Techniques

As shown in Figure 3.2 and 3.3, transistors T1 and T6 are the two-stage, common-emitter cascade amplifier. Figure 3.4 shows the two-stage, common-emitter cascade amplifier where $T_1=Q_1$ and $T_6=Q_2$.

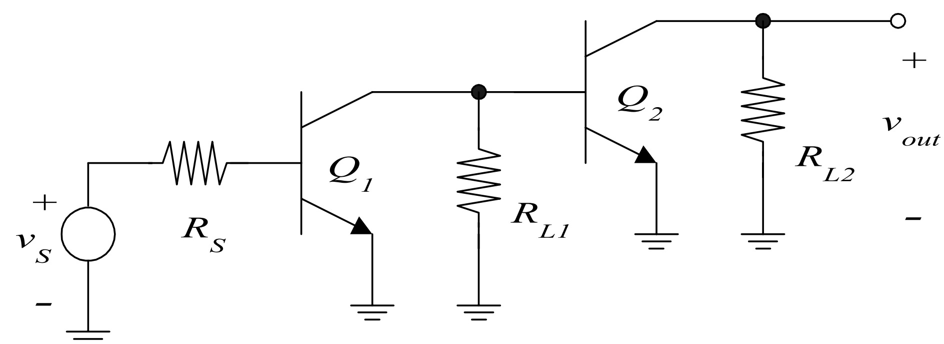

Figure 3.4 Two-stage, common-emitter cascade amplifier

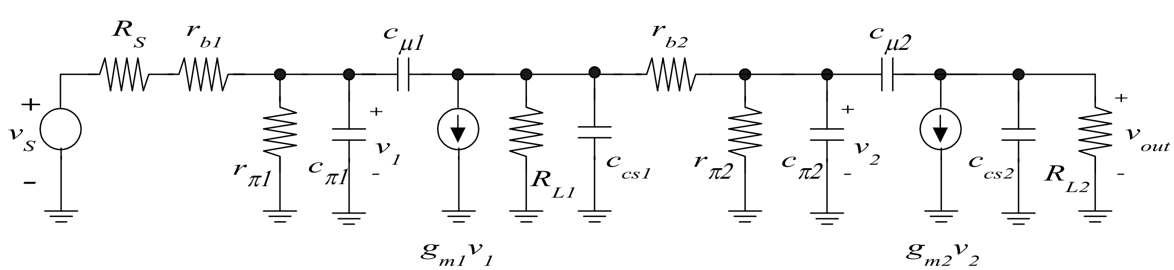

Figure 3.5 Small-signal equivalent circuit of Fig.3.4

Figure 3.5 shows the small-signal equivalent circuit of Fig. 3.4. The conventional analysis of this circuit to find the dominant pole and –3dB frequency are given by (Paul et al., 1993):

$$\omega_{-3dB} = \frac{1}{C_{\pi1}R_{\pi01} + C_{\pi2}R_{\pi02} + C_{\mu1}R_{\mu01} + C_{\mu2}R_{\mu02} + C_{cs1}R_{cs01} + C_{cs2}R_{cs02}} \tag{3.15}$$

where

$$C_{\mu1}R_{\mu01} = C_{\mu1}R_{\pi01}\left(1 + g_{m1}R_{L1eff} + \frac{R_{L1eff}}{R_{\pi01}}\right) \tag{3.16}$$

$$C_{\mu2}R_{\mu02} = C_{\mu2}R_{\pi02}\left(1 + g_{m2}R_{L2eff} + \frac{R_{L2eff}}{R_{\pi02}}\right) \tag{3.17}$$

$$C_{cs1}R_{cs01} = C_{cs1}R_{L1eff} \tag{3.18}$$

$$C_{cs2}R_{cs02} = C_{cs2}R_{L2eff} \tag{3.19}$$

The values $R_{\pi0}$ and R_{Leff} for each device can be calculated by

$$R_{L1eff} = R_{L1} // (r_{b2} + r_{\pi2}) \tag{3.20}$$

$$R_{L2eff} = R_{L2} \tag{3.21}$$

$$R_{\pi01} = r_{\pi1} // (R_{S1} + r_{b1}) \tag{3.22}$$

$$R_{\pi02} = r_{\pi2} // (R_{S2} + r_{b2}) \quad \text{where} \quad R_{S2} = R_{L1} \tag{3.23}$$

The dominant pole and –3dB frequency of the technique 1 and 2 can be modified version of an existing the dominant pole and –3dB frequency (Paul et al., 1993) where the transistors Q1 and Q2 are the transistors T1 and T6, respectively, and the loading resistance R_{L1} of Q1 is the output resistance r_o of transistors T4. At high frequencies, capacitors C_1 and $2C_1$ are all short circuits. The resistance R_{L2} of Q2 is zero. It can be seen from (3.15) that the dominant pole and –3dB frequency of Technique 1 and 2 are given by

$$\omega_{-3dB} \approx \frac{1}{C_{\pi1}r_{\pi1} + C_{\pi2}r_{\pi2} + C_{\mu1}(r_{\pi1} + r_{\pi2}) + C_{\mu2}r_{\pi2} + C_{cs1}r_{\pi2}} \tag{3.24}$$

As an example, it can be expected from (3.24) that the limited frequency $f_{-3dB} \approx 50$ MHz if $C_{\pi 1} = C_{\pi 2} = 1$ pF, $C_{\mu 1} = C_{\mu 2} = 1.1$ pF, $C_{CS1} = 1.2$ pF and $r_{\pi 1} = r_{\pi 2} = \beta r_e = 120 \times (25\ \Omega) = 3\text{k}\ \Omega$.

3.8 Conclusions

Chapter 3 proposes a possible system realization of a high-Q bandpass filter followed by two circuit realizations through Techniques 1 and 2, i.e. fully balanced, high-Q, wide-dynamic-range current-tunable Gm-C bandpass filters I and II. Technique 1 is relatively simple based on two fully balanced components, i.e. a two-input adder and a low-Q-based bandpass filter. The high quality factor Q_{HQ1} of Technique 1 is approximately equal to a typically high (>100) and constant value of the current gain β, and is, for the first time, independent of variables such as a center frequency. Possible solutions for good stability of the quality factor Q_{HQ1} with temperature have been suggested through the use of, for example, InGaP/GaAs Heterojunction Bipolar Transistors (HBTs) where the β is relatively constant. Not only can the need for additional Q-tunable circuits be greatly reduced, the sensitivity of the Q factor can be greatly improved. Technique 2 is also relatively simple based on three fully balanced components, i.e. a two-input adder, a low-Q-based bandpass filter and a differential amplifier. The high quality factors Q_{HQ2} of Technique 2 is possible through a tunable bias current I_3. In addition, center frequencies of Techniques 1 and 2 are easily tunable by a bias current I_2.

In Technique 1, the sensitivity of Q_{HQ1} to the variation of β and the sensitivities of ω_{HQ} to the variations of C_1, V_T, or I_2 are constant values from –1 to 1 and therefore, are desirably independent of parameters. In Technique 2, for very high-Q realizations (i.e. $I_3 \cong V_T/R_C$), the sensitivities of Q_{HQ2} to the variation of R_C, V_T, or I_3 are in the same order as other existing approaches whilst the sensitivities of ω_{HQ} to the variations of C_1, V_T, or I_2 are constant values from –1 to 1. In Techniques 1 and 2, for a large value of β, the sensitivity of ω_{HQ} to the variation of β is not only relatively small but also relatively constant. In addition, dynamic ranges (DRs) of Techniques 1 and 2 are potentially higher than other existing Gm-C approaches due to the use of fully balanced structure and appropriate setting of capacitors.